Machinability Of Shape Memory Alloy Using Electro Spark Erosion Process

Adam Khan M
Kalasalingam Academy of Research and Education (KARE)
Winowlin Jappes J T
Kalasalingam Academy of Research and Education (KARE)
Samuel Ratna Kumar P S (samuelrathish@live.com)
University of Johannesburg
Mashinini P M
University of Johannesburg

Original Research

Keywords: NiTi alloy, electro spark, MRR, surface topography

Posted Date: February 2nd, 2021

DOI: https://doi.org/10.21203/rs.3.rs-160831/v1

Abstract

In this research work, the nickel – titanium based shape memory alloys are machined using electro spark machining process. The influence of the input process for electro spark production is studied in detail. From the analysis, the tool wear rate (TWR), surface roughness, and material removal rate (MRR) are investigated. The intensity of the electro spark produced at minimum pulse on-time 10 μs and maximum applied voltage (60 V). Variation in MRR is wide for a minimum pulse on time with low applied voltage. The surface roughness of the machined surface is also directly influenced by the in – efficient spark produced. The copper electrode with increase pulse duration the alloy behaves like a strong conductor to transmit electrical energy between the electrode and work material. The contribution of pulse on-time is maximum for material removal and tool wear rate. However, the surface finish depends on the applied voltage of the process designed. The impact on machined surfaces, micro-cracks, electro-discharge carter's, and recast material due to electrical discharge were assessed using a scanning electron microscope and energy-dispersive X-ray spectroscopy (EDX) analysis. The experimental value shows that material removal depends on the pulse on process timings and applied voltage. Thus, by using mathematical analysis the influence of (electric discharge machining) EDM process parameters was evaluated.

Introduction

In the current research scenario, development on shape memory alloy (SMA) is in successful track. Demand for SMA is an increasing trend for many engineering components. The SMA has different element weight percentage of nickel and titanium as a binary alloy [1]. In combination with nickel and titanium, research is also available with cobalt and carbon as minor alloying elements [2]. Superior in mechanical properties and its functional quality has made shape memory alloy to be recommend for different applications [3]. It has high hardness and recommended as an imperative material for tribological applications in automobile components [4]. The application of shape memory alloy in aerospace applications has extended in different aspects [5]. Not only for engineering applications, the trail for biomedical engineering has also been simultaneously increased. Literature report on biocompatibility studies for nickel and titanium alloy is also in trending [6, 7]. The important factor in these applications are that the components will have complex and intricate profile with dimensional accuracies. It is difficult to handle with conventional manufacturing process for machining and other dimensional modifications [8]. Since, the research scope has been focused on different manufacturing techniques to process functional materials.

Machinability of nickel – titanium alloy is one of the stimuli for recent researchers. Presence of nickel and titanium elements in the alloy has high hardness. Literatures are available to discuss about conventional machining process such as turning, drilling and milling of the alloy. While machining, the plastic deformation of the alloy is tough to shear due to superior strength. Difficulties in machining SMA alloy with cutting edge is tool wear, built – up edge, surface deficiencies and the cost of production [9 – 11]. To overcome such issues with conventional process, advanced manufacturing processes are involved to

make machinability of the alloy [12]. Electro spark machining process is one of the prime techniques in advanced manufacturing process [13]. It works based on the electro spark produced between the work and the electrode. The intensity of electro spark depends up on input process parameters and the thermal conductivity of the material. Significantly, the opportunity for machining shape memory alloy is in open challenges.

In this paper, an attempt is made to machine nickel – titanium based shape memory alloy using electro spark machining process. The input process parameters such as applied voltage, pulse on time and pulse off time are varied to study the machinability of the alloy. Response on the proposed work is measured through electron microscope and material removal rate. Based on the investigation, the suggestion are given.

Experimental Procedure

It is challenging to handle shape memory alloy (SMA) with conventional manufacturing and machining processes. In this paper, the NiTi based SMA is as an investigation material having nickel (55.2%), titanium (44.5%) and carbon (0.3%) elements. The experimental investigation is performed through electro spark machining process. Schematic illustration of the electro spark machine is given in Figure 1. The machine operates with a following specification; power supply 3-phase alternating current with 415 V and 50 Hz. Maximum working current is 35 ± 2 Amp. The tool material used for electro spark production for machining SMA material is pure copper rod. The dimension of the electrode is □10mm rod and kerosene as a dielectric medium. From the experimentation, the machinability of the SMA material is studied by varying the pulse on time, pulse of time and applied voltage. Table 1 shows the input process parameters and its range used for machining SMA alloy. The responses are material removal rate (MRR), tool wear rate (TWR) and surface roughness (Ra) are measured to report on the machinability of the material. Mathematical equations used for material removal rate and tool wear rate are as follows [14 – 16, 1]:

$$Material\ removal\ rate\ (MRR) = \frac{Volume\ of\ material\ removed}{Time}\ (\text{mm}^3/\text{min}) \qquad \text{(i)}$$

$$Volume\ of\ material\ removed = \frac{\pi}{4} d^2 h\ (\text{mm}^3)$$

Where: d – diameter of the electrode (in mm), h – depth of cut (in mm) and the Time taken to remove material is in minutes.

$$Tool\ wear\ rate\ (TWR) = \frac{Volume\ of\ material\ removed}{Time}\ (\text{mm}^3/\text{min}) \qquad \text{(ii)}$$

$$Volume\ of\ material\ removed = \Delta T_w\ \rho\ (\text{mm}^3)$$

Where: ΔT_w is change in tool weight (in gram), ρ is density of electrode and Time taken for machining SMA material.

Further, the machined samples are investigated with a surface measurement device to find average surface roughness. Subsequently, the electron imaging technique for surface topography and energy dispersive spectroscope is used for elemental analysis study on machined surfaces. In addition, the influence of input parameters is evaluated using MINITAB software following the design of experimental analysis. From the results and discussion, the mechanism involved and the metallurgical transformation during the machining process is discussed in details.

Results And Discussion

Material removal rate and Surface roughness

From the experimental analysis, the amount of material removed from the SMA alloy is calculated and illustrated in the form of graph as shown in Figure 2. Graph shows the performance of electro spark process for different pulse on process timings. Results found with wide variations for 10 µs and the removal of material varied from 2.532 mm^3/min to 7.136 mm^3/min. For 3 µs, material removal found steadily increasing in trend with respect to the applied voltage. On other two conditions (6 and 9 µs) material loss is gradual variation with minimum variations. Subsequently, for 30 µs the material removal is in the range of 3.01 mm^3/min to 4.132 mm^3/min. Influence of applied voltage is less with maximum pulse on time. The variation in material removal for 30 µs has a very small variation (1 mm^3/min) compared to 10 µs (4.604 mm^3/min). While machining the electro spark induced at minimum pulse on has high intensity to fuse and vaporize the material under die sinking. Due to increase in pulse of time the intensity of the spark has prolonged to diffuse material in bulk and MRR found increased. It is inclined towards the current density, which is generated due to the discharge current [15, 16]. The accumulated discharge energy will have severe melting and evaporation of the material. However, for maximum pulse time material behavior varied and it starts to conduct the energy between the electrode and work. The presence of carbon (alloying) elements in SMA alloy has categorized the material to have high electrical conductivity. Specifically, for prolonged electro spark the presence of carbon in the SMA intended to conduct the amount of energy used. During machining the high conductivity of the material leads to transform energy (electrical conductivity) between the electrode (pure copper material) and the SMA work material [15]. It also defeats the production of electro spark and the intensity of the spark turns weak and form inefficient process. During electro spark production, the electrode or the tool used becomes vulnerable with respect the machining conditions. The tool in contact with the work will also possess slight melting and vaporization. Figure 3. indicates the measure of tool wear rate with respect to applied voltage at different pulse on and pulse of time. The behavior of the electrode tool material is varying strongly with respect to minimum pulse on time. Reflection of SMA alloy material removal is directly reflecting with the performance of copper electrode material. Uniform and linear result for maximum pulse on time noticed with tool wear. The metallurgical ion transmission and conductivity due to current density are discussed with surface topographical analysis.

The material removal and surface roughness of SMA material under electro spark machining has performed with the similar pattern. Figure 4. illustrates the measured average surface roughness value for

different pulse duration and applied voltage. As discussed in material removal, the surface roughness of the SMA material has produced results with wide range for low pulse on time (10 µs). Minimum surface roughness recorded is 1.04 µm for an applied voltage of 40V and maximum of 3.47 µm for 60 V at 3 µs (pulse off time). It has to be understood that the surface roughness found increased with respect to increase in applied voltage. This is due to the interruptions in discharge current and strikes from electro spark. On extension of pulse during electro spark, the melting of material is with highly intense and deep craters initiated. The variations in material removal is due to the low pulse on time and floatation in pulse off time. For maximum pulse on time, the material removal found uniform and gradual Similarly, the variation in surface roughness is due to the intensity of spark voltage. When applied voltage increases the material removal reveals catastrophic with maximum roughness. Since the maximum surface roughness recorded for maximum applied voltage and pulse off time. As a result, the pulse on time has played vital role in material removal and applied voltage for surface roughness. To confirm the influence of process parameters, the experimental data is evaluated through mathematical analysis.

Influence of input process parameters over MRR and Ra

The data extracted from the experimental analysis is mathematically evaluated to find the influence of input process parameters. analysis is performed through the MINITAB software with the eighteen combinations of experimental design and their corresponding results. From the analysis of experimental design (ANOVA), the influence of is process parameters is predicted and plotted in the form graph (Figure 5). It is clear to infer that the material removal is highly influenced by the pulse on time with a maximum contribution of 60.7%. Pulse off and applied voltage are less and equal in contribution (15%) for the response on material removal. While comparing the SMA alloy and copper electrode, the influence of pulse on time is severe with copper electrode. For better understanding, the electrode ion transmission at low pulse on time has high resistance and the material (tool wear) loss occurred. At the same with increase in pulse on time, the current density was diminished and act as a conducting material to transfer electrical energy from the electrode to work piece. Since the maximum contribution of 79.18% recorded for tool wear rate. In both the case (MRR and TWR), the influence of applied voltage is 6 to 8%. Similarly, for surface roughness, the intensity of electro spark in terms of applied voltage has maximum contribution of 92.4%. The significance in the research finding is that the intensity of the spark depends on the applied voltage. Based on the spark intensity, the SMA alloy melts and vaporized with the pressurized dielectric fluid. Surface profile reveals crater with strong electro spark and partially melted cast layer due to in – efficient spark. The fitness of the equation (R^2 Adj value) for the proposed experimental design is 91.9% for MRR, 97.83% for surface roughness and 93.83% for TWR.

Surface Topographical analysis

The surface morphology of the EDM process SMA alloy entirely depends on the machining parameters. Figure 6 (a) – (f). Shows SMA alloy's surface morphology image under different machining parameters such as pulse on time of 10 – 30, pulse off time of 3, 6, and 9, a voltage of 40 – 80, and Cu electrode. The performed EDM process was characterized by electro-discharge carters, recast material, and melting

point. Fewer micro-cracks occurred along the EDM machined surface, and the recast materials will attribute a quick shrinkage. These micro-cracks occur due to thermal shock stress. The electro-discharge carter and micro-crack and recast material formation will change the hardness of the machined surface [17, 18]. There is a change in machining energy with the increasing voltage, so the electro-discharge craters have become broader and more profound, contributing to evident surface roughness (Ra) in μm [18 – 20]. When the voltage increases, the electro-discharge carter's extension is high and decreases crack density. At high voltage, few micro-cracks were parallel along the machined surface. The recast material layer thickness was increased initially and then decreased with increased pulse duration, as shown in Figure 6 (c) - (d). The high pulse duration relatively will have increased electro-discharge energy. This increased electro-discharge energy will resolve and melt the material, as well as dissolve in the dielectric medium, which settles along the EDM machined surface [19]. Thus, the recast material layer thickness was widened. An extra high electro-discharge energy will have sufficient impact energy to effectively remove the molten materials and accumulated materials from the EDM machined surface by increasing the pulse duration. Thus, it will reduce the thickness of the recast material layer.

Figure 7 (a – f) represents the secondary electron (SE) image and energy-dispersive X-ray spectroscopy (EDX) analysis of the EDM machined surface of the SMA alloy. The EDX analysis shows significant elements such as Ti, Ni, C, Cu, and O in the EDM machined surface layer. Thus, it shows the EDM machined surface layer has TiO_2, TiC, Cu_{81} Ni_{19}, Cu_2O, C, and rich phase of Ni. The recast material layer consists of oxides TiO_2 and the consumed Cu electrode deposition particles, and the dissolved dielectric medium. Alidoosti et al. [19] describe the TiO_2, TiC, and Cu_{81} Ni_{19} compounds attributed to Ni and Ti atoms' great action. Due to the deposition of the consumed Cu electrode, Cu_2O and Cu_{81} Ni_{19} occurs. Also, TiC and C are the effects of the dielectric medium.

Conclusion

This research work shows the importance of knowing the impact of various machining parameters to achieve a good machining operation for nickel-titanium based SMAs. Furthermore, upon the machined surfaces of SMA, electro-discharge craters and recast materials were identified using scanning electron microscope and energy-dispersive X-ray spectroscopy analysis. From energy-dispersive X-ray spectroscopy analysis, TiO_2 oxides and the sediment particles of it's extracted Cu electrode were identified along the machined surfaces. The MRR found increased, due to the increase in pulse of time and the intensity of the spark and TWR is uniform and linear for maximum pulse on time. The minimum and maximum surface roughness registered is 1.04 – 3.47 μm at 40 – 60V. It is understood that by increasing an applied voltage and pulse timing, the surface roughness has increased. From the analysis of experimental design, material removal and tool wear rate were highly influenced by the pulse on time with a maximum contribution of 60.7% and 79.18%. Similarly, surface roughness is influenced with a very high contribution of 92.4%. Finally, the mathematical analysis proposed an optimal data with an equation for the proposed experimental design is 91.9% for MRR, 97.83% for surface roughness and 93.83% for TWR.

Declarations

Author declaration:

Ethics approval

Not applicable.

Consent to Participate

Not applicable.

Consent to Publish

Not applicable.

Authors Contributions

Adam Khan M and Samuel Ratna Kumar P S: Have made substantial contributions to conception and acquisition of data, or analysis and interpretation of data; involved in drafting the manuscript.

Winowlin Jappes J T and Mashinini P M: General supervision of the research; revising it critically for important intellectual content; have given final approval of the version to be published.

Funding

No funding was received for this work.

Competing Interests

No conflict of interest exists.

Availability of data and materials

All data generated or analysed during this study are included in this published article.

References

1. Mahendra Uttam Gaikwad et al 2019 Mater. Res. Express in press https://doi.org/10.1088/2053-1591/ab08f3
2. Soni Hargovind, Peter Madindwa Mashinini, Effects on microstructure and material properties of TiNiCo shape memory alloys, Emerging Materials Research, 9 (2), 266-271 (2020).
3. Nemat-Nasser, J.Y. Choi, W.G. Guo, J.B. Isaacs, Very high strain-rate response of a SMA shape-memory alloy, Mechanics of Materials. 37 (2005) 287 – 298.

4. Gheorghita, V., Gümpel, P., Chiru, A. et al. Future applications of Ni-Ti alloys in automotive safety systems. Int. J Automot. Technol. 15, 469–474 (2014). https://doi.org/10.1007/s12239-014-0049-z
5. Shih-Fu Ou, Bou-Yue Peng, Yi-Cheng Chen and Meng-Hsiu Tsai, Manufacturing and Characterization of NiTi Alloy with Functional Properties by Selective Laser Melting, Metals 2018, 8, 342. doi:10.3390/met8050342
6. Duerig, T.; Pelton, A.; Stockel, D. An overview of nitinol medical applications. Mater. Sci. Eng. A 1999, 273, 149–160.
7. Habijan, T.; Haberland, C.; Meier, H.; Frenzel, J.; Wittsiepe, J.; Wuwer, C.; Greulich, C.; Schildhauer, T.A.; Köller, M. The biocompatibility of dense and porous Nickel–Titanium produced by selective laser melting. Mater. Sci. Eng. C 2013, 33, 419–426.
8. L. Chen, S.F. Hsieh, H.C. Lin, M.H. Lin, J.S. Huang, Electrical discharge machining of TiNiCr and TiNiZr ternary shape memory alloys, Materials Science and Engineering A 445–446 (2007) 486–492
9. Weinert, V.Petzoldt, D.Kötter, Turning and Drilling of NiTi Shape Memory Alloys, CIRP Annals, 53(1), 2004, 65 – 58.
10. Sachin Ashok Sonawane, M.L. Kulkarni, Optimization of machining parameters of WEDM for Nimonic-75 alloy using principal component analysis integrated with Taguchi method, Journal of King Saud University – Engineering Sciences 30 (2018) 250–258. doi.org/10.1016/j.jksues.2018.04.001
11. Eren Kaya & İrfan Kaya, A review on machining of NiTi shape memory alloys: the process and post process perspective, The International Journal of Advanced Manufacturing Technology (2019) 100:2045–2087
12. Eun Sang Lee and Tae Hee Shin, An evaluation of the machinability of nitinol shape memory alloy by electrochemical polishing, Journal of Mechanical Science and Technology 25 (4) (2011) 963~969
13. Rakesh Chaudhari, Jay J. Vora, Vivek Patel, L. N. López de Lacalle, and D. M. Parikh, Surface Analysis of Wire-Electrical-Discharge-Machining-Processed Shape-Memory Alloys, Materials, 13(3), 2020, 530. doi: 10.3390/ma13030530
14. Adam Khan M, Gokul A K, Bharani Dharan M.P, Jeevakarthikeyan R.V.S, Uthayakumar M, Thirumalai Kumaran S and Duraiselvam M, Machinability of nickel based alloys using electrical discharge machining process, IOP Conf. Series: Materials Science and Engineering 346 (2018) 012044 doi:10.1088/1757-899X/346/1/012044
15. Manjaiah, S. Narendranath, S. Basavarajappa, Review on non-conventional machining of shape memory alloys, Transactions of Nonferrous Metals Society of China, 24(1), 2014, 12 – 21.
16. Velmurugan, V. Senthilkumar, S. Dinesh, D. Arulkirubakaran, Machining of NiTi-shape memory alloys-A review, Machining Science and Technology, 22 (3), 2018, 355 – 401.
17. Huang, H. Zheng, Y. Liu, Experimental investigations of the machinability of Ni50.6Ti49.4 alloy, Smart Materials and Structure, 14(5), 2005, 297-301.
18. Theisen, A. Schuermann, Electro discharge machining of nickel–titanium shape memory alloys, Materials Science and Engineering, 378(1), 2004, 200-204

19. Alidoosti, Ali Ghafari-Nazari, Fathollah Moztarzadeh, Newsha Jalali, Sina Moztarzadeh, Masoud Mozafari, Electrical discharge machining characteristics of nickel–titanium shape memory alloy based on full factorial design, Journal of Intelligent Material Systems and Structures, 24(13), 2013, 1546–1556.
20. C. Lin H, K.M. Lin, I.S. Cheng, The electro-discharge machining characteristics of TiNi shape memory alloys, Journal of Materials Science, 36(2), 2001, 399-404.

Table

Table 1: Input Process parameters and ranges used for SMA machining.

Parameter	Range	Units
Pulse on time	10 and 30	µs
Pulse off time	3, 6 and 9	µs
Voltage	40, 50 and 60	V

Figures

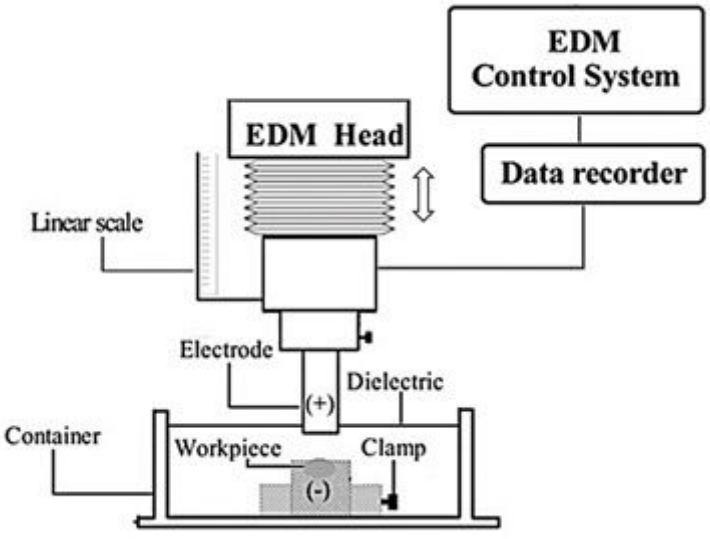

Figure 1

Schematic diagram for electro spark machining arrangements

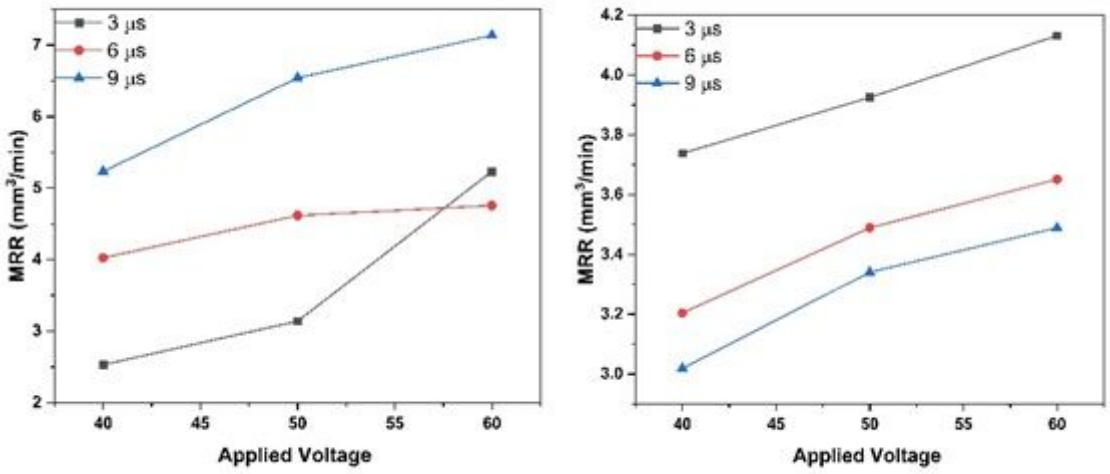

Figure 2

Graphical illustration of SMA alloy material removal with respect to pulse on / off and applied voltage

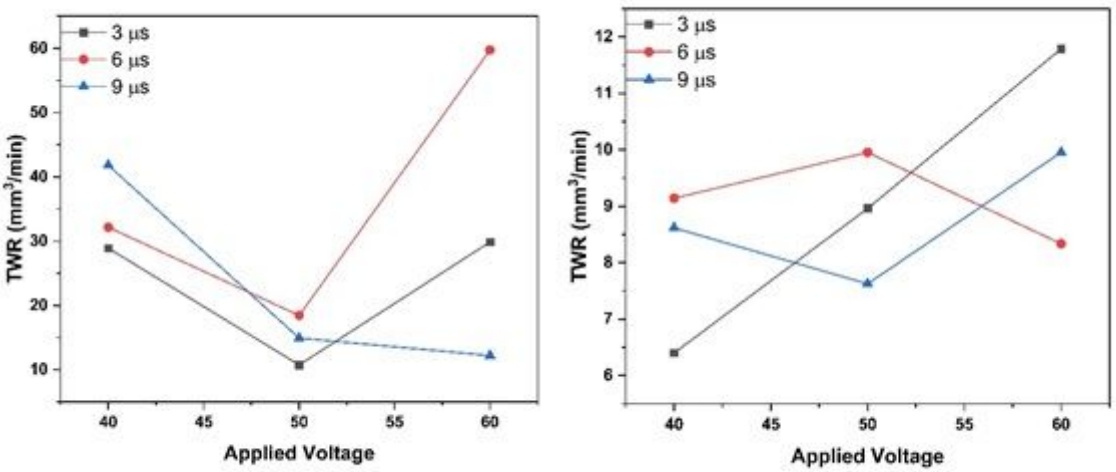

Figure 3

Tool wear rate (copper electrode) measured while machining SMA alloy through electro spark erosion method

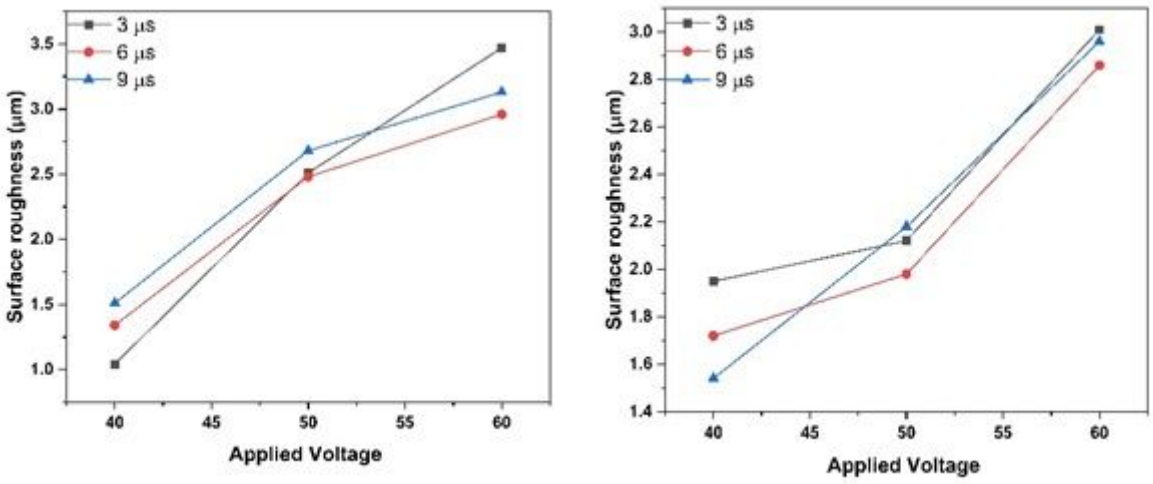

Figure 4

Average surface roughness measured on SMA alloy of electro spark machined surface

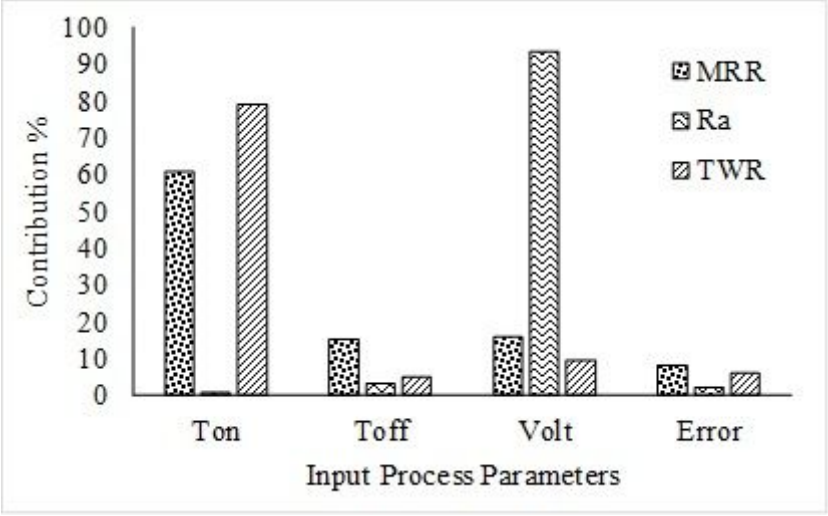

Figure 5

Average surface roughness measured on SMA alloy of electro spark machined surface

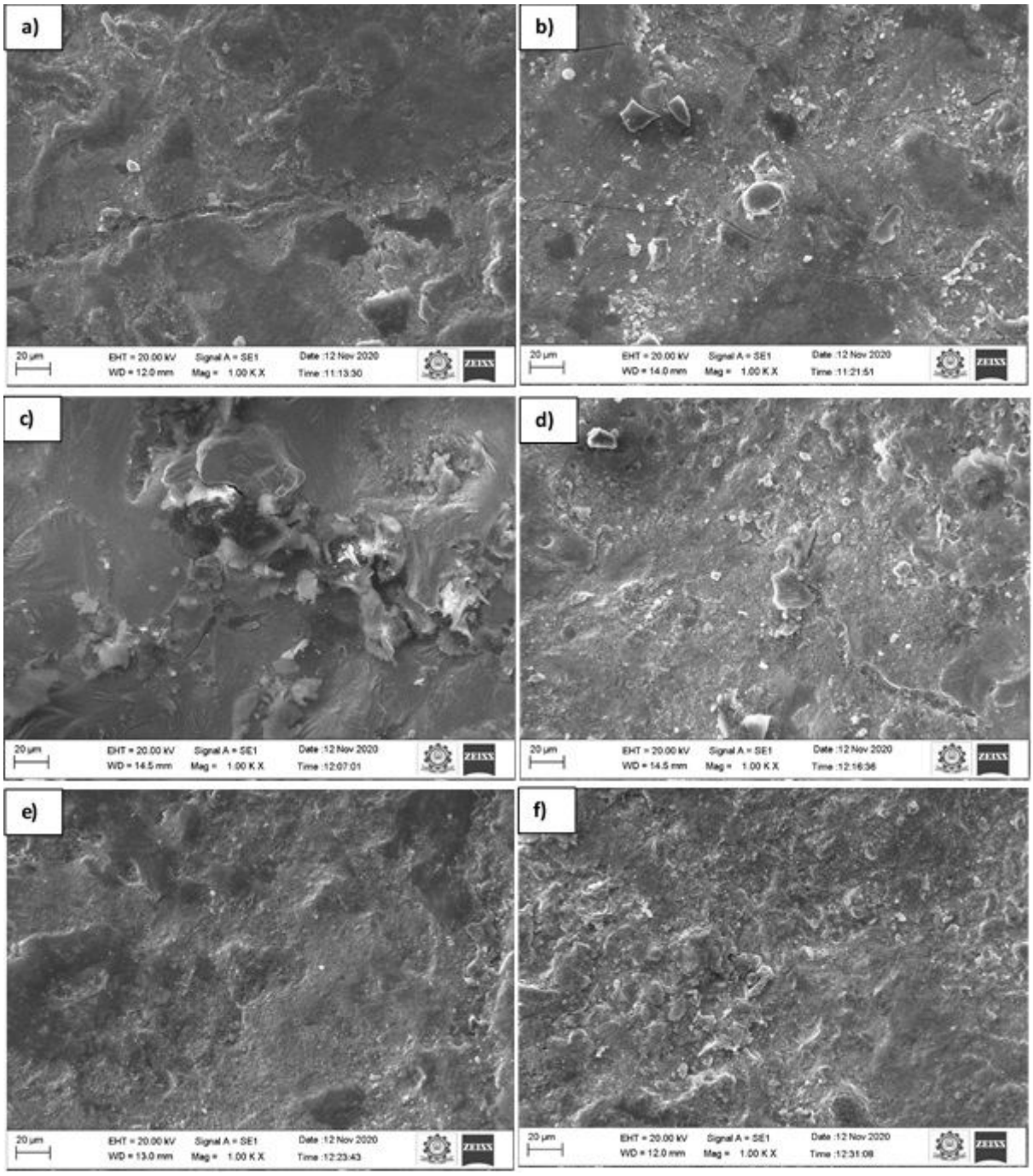

Figure 6

Secondary electron (SE) surface morphology image of NiTi alloy after the EDM process under different voltages.

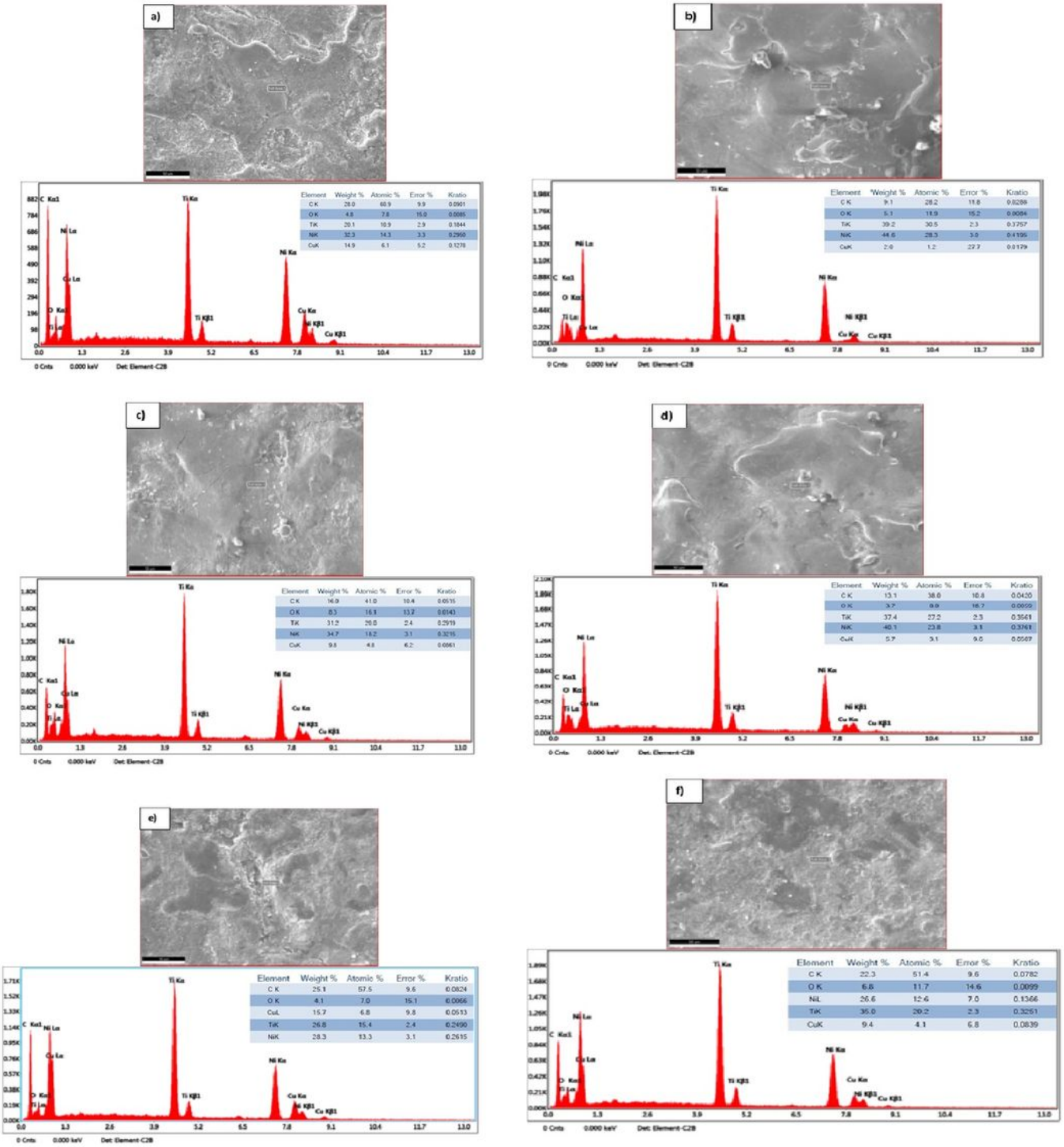

Figure 7

Secondary electron (SE) image and energy-dispersive X-ray spectroscopy (EDX) analysis of NiTi alloy after the EDM process under different voltages.